

Impact of Path Loss and Delay Spread on Base Station Cooperation

Konstantinos Manolakis, Stephan Jaeckel, Eva Salvador Marquez, Volker Jungnickel
Fraunhofer Heinrich Hertz Institute
Einsteinufer 37, D-10587, Berlin, Germany
Konstantinos.Manolakis@hhi.fraunhofer.de

Abstract—In this paper, we investigate the maximum inter-site distance (ISD) for performing joint signal processing between cooperative base stations. As a metric, we use the maximum excess delay measured at 95% point of the cumulative power delay profile from all base stations. For the distance-dependent channel parameters, we consider Greenstein’s statistical propagation model, which we extended for broadband transmissions. We extract all model parameters from 2.6 GHz multi-cell measurements in our field trial and parametrize the model at a fixed ISD. We also investigate the impact of antenna downtilt and find that when a larger downtilt is used, the rms delay spread and 95% excess delay are smaller. However, there are critical 3D effects close to the sites not included in the model. Then we consider larger ISDs and indicate how the delay parameters grow. Based on Greenstein’s model, the short cyclic prefix in LTE is hardly violated for realistic ISD at 2.6 GHz.

I. INTRODUCTION

Base station cooperation is envisioned as a promising technique for future mobile networks where the carrier frequency shall be fully reused. It reduces the mutual interference between adjacent radio cells and increases significantly the spectral efficiency [1]. In the downlink, multiple antennas at multiple base stations are considered as inputs and multiple terminals served in the corresponding cells are considered as outputs of a distributed multiple-input multiple-output (MIMO) system. Recent research has revealed that spatial multiplexing of multiple data streams is possible provided that the channel information between all transmit and receive antennas is provided and joint signal processing is performed at least at one side of the MIMO link.

Multi-carrier transmission using orthogonal frequency division multiplexing (OFDM) is a favorable scheme to manage the complexity of the required signal processing for MIMO and is standardized in the 3rd generation partnership project (3GPP) long term evolution (LTE) [2]. OFDM is well suited for transmission over frequency-selective channels, as it divides the available bandwidth in a number of orthogonal sub-channels, where each of them observes frequency-flat channel fading and can be processed separately. However, the cyclic prefix (CP) needed for sub-carrier based equalization reduces the spectrum efficiency. It is chosen little longer than the largest multipath delay in the targeted propagation environment. If multiple distributed base stations serve a terminal jointly, there are additional contributions to the overall delay statistics which might violate the CP length and create inter-

symbol interference (ISI) between successive OFDM symbols.

There is previous work about the dependence of channel delay spread from the path gain and thus the propagation distance. In [3] it was found that the delay spread as well as its standard deviation increase with distance and deep shadow fading in urban scenarios. An overview of the state of the art in cooperative MIMO channel modeling can be found in [4], where new challenges and open issues are addressed.

In this paper, we consider the impact of base station (BS) cooperation on the overall delay statistics in a realistic deployment scenario. We seek for an answer to the question what distance is allowed between cooperative base stations without violating a given CP. As a starting point, we use a distance-dependent statistical propagation model originally introduced by Greenstein et al. [5], which describes also the correlation between path gain and delay spread. We parametrize this model based on coherent multi-cell channel measurements from our LTE-Advanced field trial in Berlin [6–8]. Therefore, we extract the distance dependencies of path loss, shadow fading and delay spread as well as their correlation at a carrier frequency of 2.6 GHz in an urban macro-cell scenario.

We illustrate that Greenstein’s model predicts the delay statistics properly at least at larger distances from the BS. Close to the BS, however, we observe significant deviations from the predicted statistics if the downtilt is set so that the main beam touches the ground at 0.9 times the inter site distance (ISD). With a downtilt of 0.33 times the ISD, as recommended by 3GPP for LTE-Advanced (see [9]), the overall delay statistics is mostly due to the overlap region covered jointly between adjacent sites, where Greenstein’s model is more appropriate. Thus we can increase the ISD and predict the delay statistics by using our parametrized propagation model. Our results indicate that BS cooperation in LTE-Advanced is feasible for distances up to 1.7 km between the sites at 2.6 GHz without violating the short CP.

The paper is organized as follows. In Section II, Greenstein’s model is reviewed and extended for broadband multi-cell transmissions. In Section III, our measurement setup and the parameter extraction routines are described. Section IV presents the extracted parameters and discusses the scope of the model by comparing prediction and measurement results. Furthermore, the parametrized model is used for predicting the delay statistics in larger cells. Finally, conclusions are discussed in Section V.

II. THE RADIO CHANNEL MODEL

A. Single-Link Narrow-Band Channel Model

Greenstein [5] states three fundamental conjectures about the channel delay spread:

- the rms delay spread is lognormal at any distance
- it's median value increases with distance
- the delay spread tends to grow in deep shadow fading

The last conjecture is very important as it suggests that dispersion is larger in case of deep shadow fading, when the signal to noise ratio (SNR) is already weak. In [5] physical arguments that support these conjectures are explained and confirmed by the existing literature. Finally, a mathematical model for the joint statistics of average path gain and rms delay spread is proposed. Parameters are specified for various environments in [5].

The path gain is given by:

$$g = G_1 d^{-\gamma} x, \quad (1)$$

where d is distance in kilometers, G_1 is the median value of path gain g at a reference distance of $d = 1$ km, γ is the path loss exponent (usually between 2.5 and 4) and x is a lognormal variate at distance d . Specifically, $X = 10\log(x)$ is a Gaussian random variable with zero mean and a standard deviation σ_x .

The median value of the rms delay spread τ_{rms} increases according to distance with an exponential factor ϵ . The rms delay spread at distance d is given by

$$\tau_{rms} = T_1 d^\epsilon y, \quad (2)$$

where T_1 is the median value of τ_{rms} at $d = 1$ km, the exponent ϵ lies between 0.5 and 1.0, and y is a lognormal variable. Specifically, $Y = 10\log(y)$ is a Gaussian random variable at distance d , which has zero mean and a standard deviation σ_y .

The delay spread is correlated by a negative correlation coefficient with the shadow fading gain. If strong channel taps, which usually arrive at early time instants, are blocked by large objects (negative shadowing gain), τ_{rms} is expected to grow. Hence, the correlation between g and τ_{rms} is described by

$$\mathcal{E}(XY) = \rho \sigma_x \sigma_y. \quad (3)$$

Here, ρ is the correlation coefficient between the two Gaussian variables X and Y and $\mathcal{E}(\cdot)$ denotes the expectation operator. According to the model, large τ_{rms} are associated with smaller g values, ρ should thus be negative; a value of $\rho = -0.75$ was proposed in [5] for all types of environments.

B. Multi-Link Broadband Channel Model

The channel model of Section II-A was initially introduced for narrow-band radio channels, where the sampling time is in the same order of magnitude or larger than τ_{rms} . This assumption is not valid for broadband systems like LTE, where the sampling time is significantly shorter. Therefore, we have to introduce a power delay profile (PDP). Our assumption is that the PDP follows an exponential decay, which is well

accepted for cellular radio channels [10]. Consequently, the received power p at distance d can be expressed by multiplying the path gain g (including shadow fading variations) with a unitary PDP p_u according to

$$p(d, t) = g p_u(\tau_{rms}, t) = \frac{g}{\tau_{rms}} e^{-\frac{t}{\tau_{rms}}}, \quad (4)$$

where g and τ_{rms} are random variates that depend on the distance d and are given by (1) to (3) and t denotes the time-delay domain. The PDP of the received signals that are radiated from N_t distributed transmit antennas is expressed by the sum of the PDP of the single links p_i :

$$P(d, t) = \sum_{i=1}^{N_t} p_i(d_i, t - t_i) = \sum_{i=1}^{N_t} \frac{g_i}{\tau_{rms,i}} e^{-\frac{t-t_i}{\tau_{rms,i}}}. \quad (5)$$

The time-shift $t_i = d_i/c$ to the i^{th} transmit antenna is calculated with respect to the closest base station, which means that the first path that is received by the mobile user at the time $t = 0$ arrives from the closest base station; c is the speed of light.

III. MULTI-CELL MEASUREMENTS

We have set up a multi-cell testbed with 3 multi-sector sites in the city center of Berlin, Germany. These BSs are placed on top of the Heinrich Hertz Institute (HHI), the main building of the Technical University of Berlin (TUB) and the Telefunken Tower Deutsche Telekom Laboratories (TLabs) as seen in Fig. 1. Detailed information on this system are available in our publications [7, 11, 12]. A precise time reference is available using an advanced global positioning system (GPS) receiver at each site and the whole radio network is synchronized to the one pulse per second (1PPS) signal. In conjunction with our coordinated multi-point (CoMP) experiments, so called channel state information (CSI) reference signals were defined to identify the channels to each of the BSs. Each BS is identified by a pilot comb in frequency domain and we apply a cyclic shift of the comb along the frequency axis by an integer number of sub-carriers where the shift identifies the cell. For identifying multiple antennas in each cell, we have used four consecutive OFDM symbols where another orthogonal sequence is transmitted for each antenna [13]. In this way, we have realized a distributed, but fully phase-coherent channel sounder for up to 6 cells.

We use +18 dBi BS antennas from Kathrein with two cross-polarized ports $\pm 45^\circ$ at the transmitter. The downtilt for all BSs was first set such that the beam hits the ground at a distance of 450 m, which corresponds to 0.9 times the ISD. In a second measurement, the downtilt was set so that the beam hit the ground at 0.33 times the ISD, as explained in Section I. Measured values for the 95% excess delay are shown on the maps in Fig. 1 and 2 for both downtilts. Additional measurement parameters are available in Table I.

At the receiver side, we use our test terminal which is synchronized over the air. The mobile terminal (MT) detects the CSI reference signals (CRS) and converts them into an Ethernet packet stream as described in [12]. This packet data

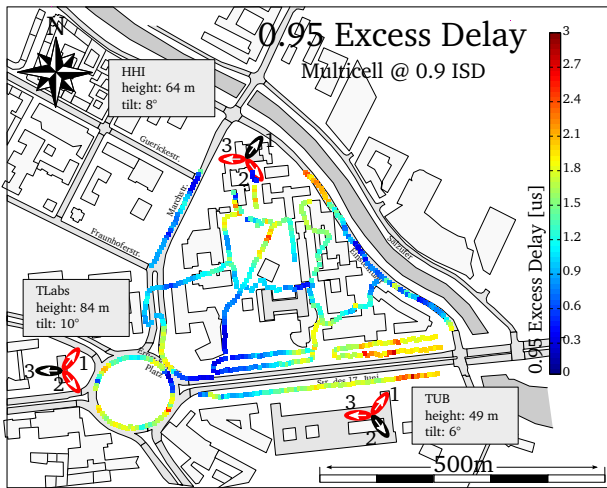


Fig. 1. Multi-cell 95% excess delay measurements. The main beam of antennas hits the ground at 0.9 times the inter-site-distance.

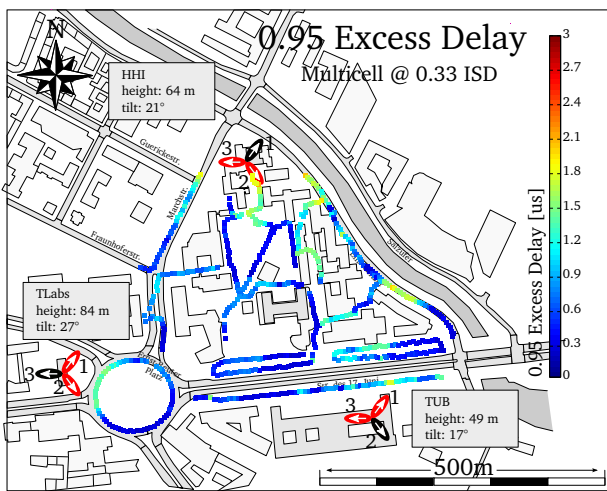


Fig. 2. Multi-cell 95% excess delay measurements. The main beam of antennas hits the ground at 0.33 times the inter-site-distance.

stream is tapped at the terminal and recorded using a notebook computer. The terminal performs coarse timing adjustment with respect to the OFDM CP. As a result, the mean multi-cell delay is measured and the impulse response is placed according to the CP.

TABLE I
MEASUREMENT PARAMETERS

Parameter	Value
Center frequency	2.68 GHz
Bandwidth (B)	18.36 MHz
No. of pilots (N)	144
MIMO capabilities	2x2 per BS
No. of BSs	6 (up to 12x2 links)
CSI update interval	10 ms
Maximal speed	2.8 m/s \approx 10 km/h
Inter site distance	\approx 500 m
BS Tx power	36.5 dBm
MT noise floor	-95 dBm

The import filter extracts a $2 \times 12 \times 144$ channel tensor for each 10 ms of the recorded packet stream. The dimensions correspond to the number of receive antennas, the number of transmit antennas and the number of pilots, respectively. The 144 channel coefficients of each Tx-Rx link can be seen as

$$\mathbf{y}_n = \mathbf{h}_n + \mathbf{v}_n, \quad n \in \{1, 2, \dots, 144\} \quad (6)$$

where \mathbf{y} is the observation (or measurement) of the broadband radio channel \mathbf{h} in frequency domain at N fixed pilot positions ν_n . These pilot positions are not equidistant in our system. \mathbf{v} is the estimation error, which is assumed to be additive white Gaussian noise (AWGN). We now use the preprocessing technique described in [8, 14] to extract the contributing multipath components. Essentially, the preprocessing calculates all parameters α and ϕ and τ which sum up to

$$\tilde{\mathbf{h}}_n = \sum_{l=1}^L \alpha_l \cdot e^{j\phi_l} \cdot e^{-2\pi j \cdot \tau_l \cdot B \cdot \nu_n} \quad (7)$$

where α_l is the amplitude, ϕ_l is the phase and τ_l is the delay of each multipath component. These parameters are the input for all following evaluation steps. Due to the processing, $\tilde{\mathbf{h}}$ has a SNR which is approximately 6 dB better than in \mathbf{y} since a significant part of the noise can be removed.

We calculate the shadow fading according to T.S. Rappaport [10]. The instantaneous path gain is first estimated from the preprocessed data by averaging all signal components over all transmit and receive antennas of one sector

$$g = \frac{1}{n_t n_r} \cdot \sum_{t=1}^{n_t} \sum_{r=1}^{n_r} P_{r,t} \quad P_{r,t} = \sum_{l=1}^L \alpha_{l,r,t}^2 \quad (8)$$

where g is the total power of a PDP. Power values for the two sectors of each site are averaged. The resulting values are then additionally averaged over segments of 5 m length to remove small scale fading effects which results in a total of 692 measurement values per BS. The shadow fading (1) in logarithmic notation notes

$$g^{dB}(d) = G_1^{dB} + \gamma \cdot 10 \log_{10}(d) + X \quad (9)$$

We calculate G_1^{dB} and γ by linearly fitting the measured data to the linear slope and then calculating the remaining variance.

The rms delay spreads are calculated by

$$\tau_{rms} = \sqrt{\sum_{l=1}^L \frac{\alpha_l^2}{P_t} \cdot \tau_l^2 - \tau_m^2} \quad \tau_m = \sum_{l=1}^L \frac{\alpha_l^2}{P_t} \cdot \tau_l \quad (10)$$

with τ_l as the delay- and α_l^2 the power of the l^{th} tap. τ_m is the mean delay and P_t is the total power. Again, we calculated the parameters T_1 and ϵ by transforming (2) into logarithmic domain and linear fitting.

At that point it has to be mentioned, that measurements from positions closer than 210 m to the BS were excluded from the evaluation. At these positions large propagation delays due to multiple reflexions on surrounding buildings were observed, while the direct signal was attenuated by the Tx antenna pattern. Such critical effects could only be captured by a 3D

TABLE II
PARAMETERS ESTIMATED FROM MEASUREMENT

Parameter	Estimated Value (HHI/TUB/TLabs)
Average path gain (G_1)	107.4 / 126.9 / 106.6 [dB]
Path loss exponent (γ)	2.0 / 6.3 / 3.0
Median of τ_{rms} (T_1)	0.4 / 0.3 / 0.3 [μ s]
Exponent ϵ	0.5 / 0.2 / 0.2
Variance σ_x	5.5 / 7.8 / 6.9 [dB]
Variance σ_y	1.7 / 1.8 / 1.5 [dB]
Correlation coefficient (ρ)	-0.7 / -0.3 / -0.6

channel model and were thus excluded here. All parameters estimated from measurements are listed in Table II.

IV. STATISTICAL EVALUATION AND RESULTS

First we validate our propagation model by parameterizing it and comparing predictions with measurements. We study the impact of antenna downtilt and look into the cases where the main beams hit the ground at 0.9 and 0.33 times the ISD. Finally, we increase the distance between the base stations for predicting the delay statistics according to our model.

Fig. 3 illustrates the cumulative distribution function (CDF) of the τ_{rms} for the multi-cell channel. The black curve shows the measured values for 0.9 times ISD antenna downtilt, while the blue curve for 0.33 times ISD. These values were taken from the route shown in Fig. 1. It is observed that by deploying a larger downtilt, significantly smaller rms delay values can be realized. The illuminated region in the cell is then more close to the BS and scattered signals have less delay. The statistics shown by the dashed red line are mostly due to the overlap region covered jointly between adjacent sites.

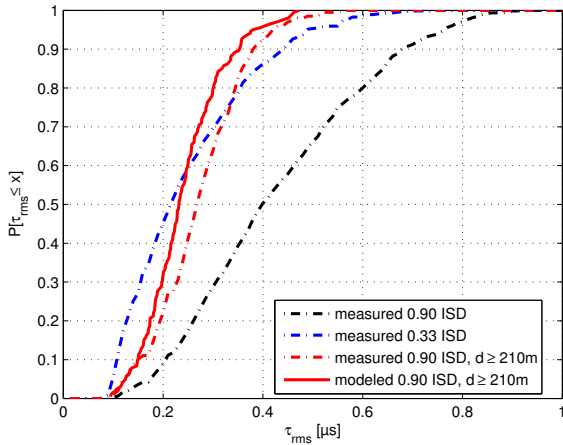


Fig. 3. Multi-cell rms delay spread τ_{rms} . The main beam of antennas hits the ground at 0.9 or 0.33 times the inter-site-distance. Model predicts well for positions at least 210 m away from the base stations.

In the next step, a multi-cell simulation environment with an ISD $d_{ISD}=500$ m is used an MT are placed on the same positions as in the measurement, as shown in Fig. 1. Independent channels are generated for the HHI, TUB and TLabs links by using the channel model as in (1) to (3) and

parameters listed in Table II. Evaluation of τ_{rms} is performed over 5000 statistically independent realizations. The τ_{rms} is calculated according to (10). The model prediction leads to the solid red line in Fig. 3, which is actually not far from the measured (dashed) line.

Fig. 4 illustrates the CDF of the τ_{95} , i.e. the 95-percentile of the cumulative PDP, that limits the signal to interference and noise ratio (SINR) contribution of the ISI to 13 dB. For the same measurement and simulation scenarios like τ_{rms} , results run into similar observations. The model predicts the expected delay parameters quite precisely, only slightly more optimistic.

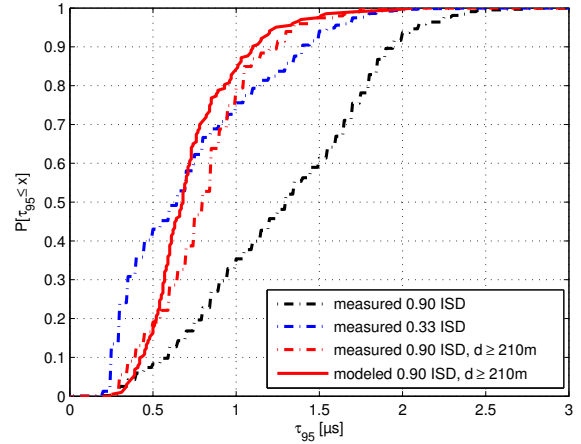


Fig. 4. Multi-cell 95% excess delay τ_{95} . The main beam of antennas hits the ground at 0.9 or 0.33 times the inter-site-distance. Model predicts well for positions at least 210 m away from the base stations.

Finally, we use the model for predicting the delay statistics for larger ISD (d_{ISD}). Channel parameters from Table II and uniform user allocation is assumed within the region defined by the three BS. Fig. 5 and Fig. 6 illustrate the τ_{rms} and τ_{95} respectively for $d_{ISD} = 500, 1000$ and 1732 m (maximum distance according to LTE [2]). It can be observed, that even in for the maximum ISD, τ_{95} exceeds the short CP length of 4.7μ s in LTE in less than 5% of the cases.

V. CONCLUSIONS AND DISCUSSION

We performed multi-cell broadband channel measurements in our testbed and studied the impact of antenna downtilting on the channel delay statistics. It was found that when using a larger downtilt, significantly smaller channel delay spreads can be realized. We extended Greenstein's statistical propagation model for covering broadband transmission from distributed base stations. Based on measured data from our field trial we parametrized the model and compared measurements with simulations. The model was verified in terms of rms delay spread and 95% excess delay. Despite of using a 2D model in a 3D setup, it predicts the delay parameters in the multi-cell case quite precisely at least at larger distances from the base stations. Close to the base stations, however, we observe deviations from the predicted statistics if the downtilt is set

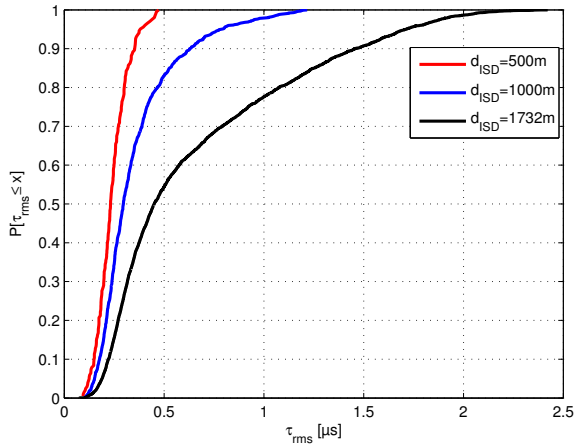


Fig. 5. Predicted multi-cell rms delay spread τ_{rms} for larger inter-site-distances and uniform user allocation between the base stations.

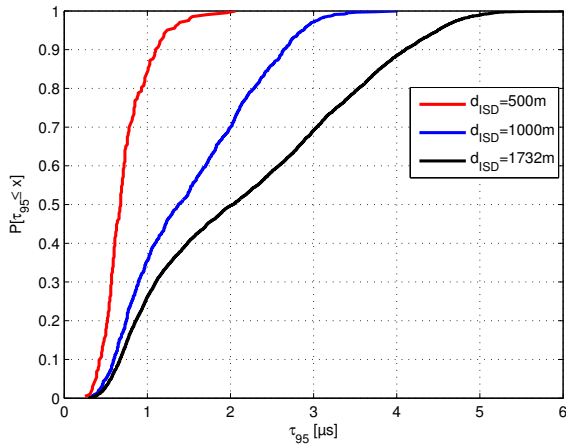


Fig. 6. Predicted multi-cell 95% excess delay τ_{95} for larger inter-site-distances and uniform user allocation between the base stations.

in a way that the main beam touches the ground at 0.9 times the inter-site-distance (small downtilt). With a larger downtilt set to 0.33 times the ISD, the overall delay statistics is mostly due to the overlap region covered jointly between adjacent sites, where the model is more appropriate. Finally we consider larger ISDs and predict the delay statistics by using our parametrized propagation model. Our results indicate that base station cooperation in LTE-Advanced is feasible for distances up to 1.7 km between the sites at 2.6 GHz without violating the short cyclic prefix.

ACKNOWLEDGMENT

The authors would like to thank the German Ministry of Education and Research (BMBF) for funding this work through the national research project EASY-C (Enablers of Ambient Services and Systems Part C – Wide Area Coverage).

REFERENCES

- [1] M. Karakayali, G. Foschini, and R. Valenzuela, "Network coordination for spectrally efficient communications in cellular systems," *IEEE Wireless Commun. Mag.*, vol. 13, pp. 56–61, 2006.
- [2] 3GPP LTE, *E-UTRA and E-UTRAN – Overall description (Release 10)*, Std., June 2010.
- [3] E. Sousa, V. Jovanovic, and C. Daigneault, "Delay spread measurements for the digital cellular channel in toronto," *IEEE Trans. Veh. Technol.*, vol. 43, no. 4, pp. 837–847, 1994.
- [4] C.-X. Wang, X. Hong, X. Ge, X. Cheng, G. Zhang, and J. Thompson, "Cooperative mimo channel models: A survey," *Communications Magazine, IEEE*, vol. 48, no. 2, pp. 80–87, 2010.
- [5] L. Greenstein, V. Erceg, Y. Yeh, and M. Clark, "A new path-gain/delay-spread propagation model for digital cellular channels," *IEEE Trans. Veh. Technol.*, vol. 46, no. 2, pp. 477–485, 1997.
- [6] S. Jaeckel, L. Thiele, A. Brylka, L. Jiang, and V. Jungnickel, "Intercell interference measured in urban areas," *Proc. IEEE ICC '09*, 2009.
- [7] V. Jungnickel, M. Schellmann, L. Thiele, T. Wirth, T. Haustein, O. Koch, E. Zirwas, and E. Schulz, "Interference aware scheduling in the multiuser MIMO-OFDM downlink," *IEEE Commun. Mag.*, vol. 47, pp. 56–66, 2009.
- [8] S. Jaeckel, L. Thiele, and V. Jungnickel, "Interference limited MIMO measurements," *Proc. IEEE VTC '10 Spring*, 2010.
- [9] L. Thiele, T. Wirth, K. Brner, M. Olbrich, V. Jungnickel, J. Rumold, and S. Fritze, "Modeling of 3D field patterns of downtilted antennas and their impact on cellular systems," *Proc. WSA '09*, 2009.
- [10] T. Rappaport, *Wireless Communications. Principles and Practice*, 2nd ed. Prentice Hall, 2002.
- [11] V. Jungnickel, L. Thiele, T. Wirth, *et al.*, "Coordinated multi-point trials in the downlink," *Proc. IEEE Globecom Workshops '09*, 2009.
- [12] V. Jungnickel, A. Forck, S. Jaeckel, F. Bauermeister, S. Schiffermueller, S. Schubert, S. Wahls, L. Thiele, T. Haustein, W. Kreher, J. Mueller, and H. D. G. Kadel, "Field trials using coordinated multi-point transmission in the downlink," *Proc. IEEE PIMRC '10 WDN-Workshop*, 2010.
- [13] V. Jungnickel, K. Manolakis, L. Thiele, T. Wirth, and T. Haustein, "Handover sequences for interference-aware transmission in multicell MIMO networks," *Proc. WSA '09*, feb 2009.
- [14] S. Jaeckel and V. Jungnickel, "Estimating MIMO capacities from broadband measurements in a cellular network," *Proc. EUCAP '10*, 2010.